Anais da Academia Brasileira de Ciências (2007) 79(3): 503-517
(Annals of the Brazilian Academy of Sciences)
ISSN 0001-3765
www.scielo.br/aabc

Quantification of porosity evolution from unaltered to propylitic-altered granites: the ^{14}C-PMMA method applied on the hydrothermal system of Lavras do Sul, Brazil

EVERTON M. BONGIOLO[1], DANIELA E. BONGIOLO[1], PAUL SARDINI[2], ANDRÉ S. MEXIAS[3], MARJA SIITARI-KAUPPI[4], MÁRCIA E.B. GOMES[3] and MILTON L.L. FORMOSO[3]

[1]Programa de Pós Graduação em Geociências da UFRGS, Instituto de Geociências
Av. Bento Gonçalves 9500, 91501-970 Porto Alegre, RS, Brasil
[2]UMR 6532 CNRS HYDRASA, Université de Poitiers, 40 Avenue du Recteur Pineau, 86022 Poitiers, France
[3]UFRGS, Instituto de Geociências. Av. Bento Gonçalves 9500, 91501-970 Porto Alegre, RS, Brasil
[4]Laboratory of Radiochemistry, Department of Chemistry, PO Box 55, 00014, University of Helsinki, Finland

Manuscript received on September 14, 2006; accepted for publication on January 31, 2007;
contributed by MILTON L.L. FORMOSO*

ABSTRACT

This work is an application of the ^{14}C-Polymethylmethacrylate method to compare the porosity evolution between unaltered and propylitic-altered granites, using samples from Lavras do Sul region, Brazil. This method, when coupled with optical and electronic petrography has the advantage over other methods to provide the quantification and identification of total and local porosity of rocks. From petrographic observations, different kinds of porous zones were identified and quantified (microfractures, grain boundaries, alteration of minerals, etc). Results show that unaltered granites have 0.5 to 0.6% porosity and propylitic-altered ones have 1.7 to 1.8% porosity, even between samples with different textures. Porosity of altered rocks increases mainly due to higher porosity of neoformed chlorite, calcite, sericite and microfractures. Field observations show that later phyllic alteration halos are wider in equigranular than in porphyritic granites, which could not be explained by different original porosity between those rocks. The observed differences of phyllic halos diffusion were controlled by structural and fluid/rock ratio variations between the equigranular and porphyritic granitic facies during the later hydrothermal stage.

Key words: porosity quantification, ^{14}C-PMMA method, granite porosity, hydrothermal alteration, propylitic alteration, Lavras do Sul.

INTRODUCTION

Methodologies for rock porosity quantification like water impregnation, mercury injection, fluorescent resin impregnation and gas adsorption in different kinds of rocks have been developed in the last decades (Dubois et al. 1998, Schild et al. 2001, Yue et al. 2004). These methods however, have reasonable resolutions only for total rock porosity. The ^{14}C-Polymethylmethacrylate (^{14}C-PMMA) method has the advantage over those methods because it provides also the porosity quantification of selected areas of the rock surface (Hellmuth et al. 1993). When coupled with petrographic data and image analysis, it is possible to recognize the petrophysical characteristics of its associated sites (Oila et al. 2005, Sardini et al. 2006).

The recognition and quantification of rock porosity are important for the following reasons (Schild et al. 2001): (1) evolution (propagation and coalescence) of microcracks controls the mechanical behavior of brittle

*Member Academia Brasileira de Ciências
Correspondence to: Everton Marques Bongiolo
E-mail: embongiolo@hotmail.com

regimes; (2) porous zones are pathways for fluid flow and solute diffusion and (3) orientation of microfissures controls the anisotropy of petrophysical and mechanical properties of rocks that can indicate stress regimes. In hydrothermal systems, porosity quantification of altered and unaltered rocks can be used as a tool for prevision of fluid/rock ratio and for recognition and quantification of pathways controlling hydrothermal alteration.

The Lavras do Sul Gold Mining District (LD) comprises hydrothermally altered Au-Cu (± Pb, Zn, Ag)-bearing prospects hosted in Neoproterozoic granitic and volcanogenic sequence, located near the town of Lavras do Sul, Rio Grande do Sul State (RS), southernmost Brazil (Fig. 1). The major gold mineralizations (0.4 to 5 ppm) are located in N40°E to E–W quartz + dioctahedral phyllosilicates + pyrite (± chalcopyrite) veins and breccia and their related alteration halos. These highly altered and deformed zones are associated to an alteration stage (phyllic alteration) that superimposes initially unaltered and propylitic (pervasive alteration) altered rocks.

The granitic complex which hosts the mineralizations is characterized by a reverse zonation of its geochemical and petrographic features, called central, transitional and border facies (Nardi and Lima 1985). The central facies comprises shoshonitic rapakivi coarse-grained porphyritic granodiorites and monzogranites, while the border facies hosts mainly alkaline coarse-grained equigranular perthite granites. The transitional facies comprises textural and geochemical hybrid rocks (monzo and syenogranites) generated by partial assimilation of the central facies by the border one (Nardi and Lima 1985). The occurrence of microgranular mafic enclaves (MME) attests a coeval mafic magmatism with both central and border granitoids (Nardi and Lima 2000), besides swarms of enclaves are more likely found in the transitional and border granitic facies.

It is known from field observations and borehole descriptions (E.M. Bongiolo, unpublished data) that diffusion of hydrothermal alteration halos around veins (phyllic alteration) is quite different between the granitic facies. Perthite granites from border facies have commonly wider halos (up to 40 m width) than rapakivi granites from the central facies (< 10 m width), although phyllic alteration was probably produced at the same time in both facies, as they have similar 595 ± 5 Ma magmatic age (Remus et al. 2000) and structural orientation of later mineralized veins associated to phyllic alteration.

The aims of the present contribution are (1) to compare the evolution of porosity between unaltered and propylitic-altered granitic rocks using samples from Lavras do Sul area and (2) to test the influence of primary porosity of rocks on the diffusion (width) of later phyllic alteration halos around veins from different granitic facies. The ^{14}C-polymethylmethacrylate (^{14}C-PMMA) method, coupled with detailed petrographic and digital image processing studies were carried out to identify and quantify the micrometer to decimeter porosity heterogeneities of rocks from central and border granitic facies and to compare the obtained results with field data.

MATERIALS AND METHODS

It was selected four granitic rock samples of drill cores from Bloco do Butiá (sample A) and Valdo Teixeira (samples C and D) prospects and of a surface quarry from Cerrito (sample B) prospect (Fig. 1B).

Samples A and B represent original or near unaltered rocks with contrasting compositions and textures (border and central granitic facies respectively) that hosts different alteration halos width of later phyllic alteration. They were collected in zones where fractures and faults are not observed. Samples C and D represent available boreholes comprising propylitic-altered rocks (border granitic facies) of contrasting texture, i.e. associated to an intermediate (pervasive) alteration stage between unaltered and highly altered rocks. They were collected in altered zones near structurally controlled quartz veins from Valdo Teixeira prospect, but with weak or no influence of later alteration halos.

THE ^{14}C-POLYMETHYLMETHACRYLATE (^{14}C-PMMA) METHOD

The ^{14}C-PMMA method developed by Hellmuth et al. (1993) consists in sample impregnation with ^{14}C-MMA under vacuum, polymerization by irradiation and autoradiography of sample surface. A bidimensional (2D) porosity image is obtained and optical density and porosity calculations were performed on samples using digital image processing techniques.

The methylmethacrylate (MMA) monomer is a po-

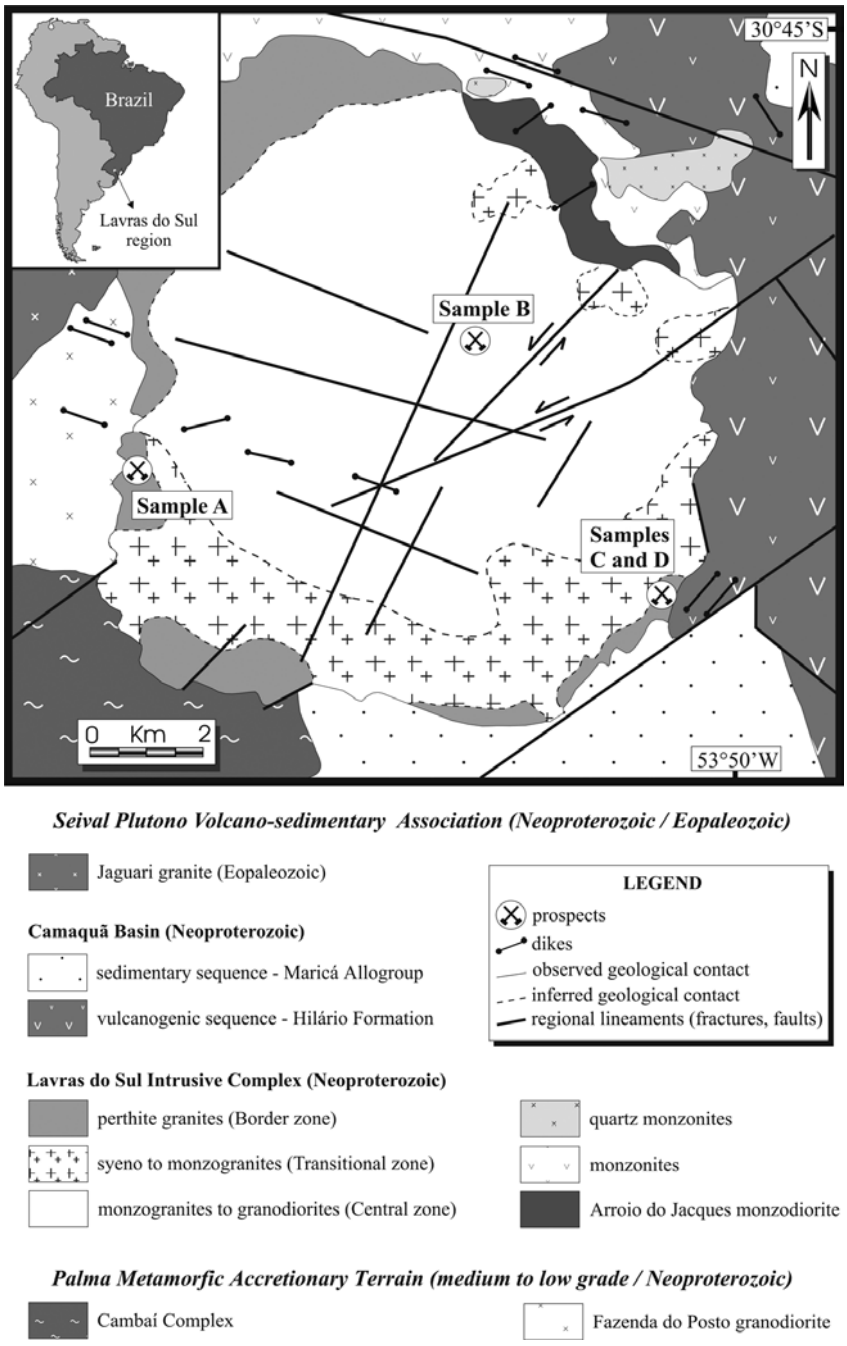

Fig. 1 – Simplified geological map of the Lavras do Sul region. Modified from Gastal and Lafon (1998). Sampling was performed in the following prospects: Bloco do Butiá (sample A), Cerrito (sample B), and Valdo Teixeira (samples C and D).

lar molecule with low viscosity (0.00584 Pa s at 20°C) and small size (100.1 g/mol) when compared to the water molecule, which allows an effective penetration in the rock porous spaces. The ^{14}C low-energy (maximum 155 keV) and its 5360 years half-life yields good autoradiographic resolutions for rocks submitted to long time impregnation.

The core samples were sawed and dried in a vacuum chamber (T = 90 to 114°C) during 10 days. The drying process is very important, because the MMA molecule

has a hydrophobic characteristic that inhibits its complete infiltration in rocks when water is present. This step was followed by the impregnation of samples with ^{14}C-MMA in the same vacuum chamber during 21 days. After that, the ^{14}C-MMA impregnated in samples was polymerized (fixed in the rock matrix) during 8 days, which consists in γ-ray irradiation (total dose: 77 kGy) using a ^{60}Co source. The initial concentration of the ^{14}C-MMA tracer used in this study was 0.5 MBq/ml. Thin sections of impregnated rock fragments were produced for petrographic observations of the similar areas and to obtain an estimative of the volume (%) of mineral phases present in each sample by point counting (1500 points). A better quantification of mafic mineral contents in exactly the same areas used for porosity quantification of unaltered rocks was performed digitally on JPEG images after selective staining techniques (see below) using Adobe Photoshop® software. The main petrographic characteristics and the mineral content in each sample are summarized on Table I. The sawn surface of rock samples was polished (1/4 μm) and cleaned ultrasonically for 3 minutes to obtain very plane surfaces before to perform the autoradiography exposition. After performed the autoradiography, the plane surfaces were covered with carbon to obtain additional petrographic observations directly on the rock, using a Jeol JSM-5800 Scanning Electron Microscope (SEM) equipped with an EDS quantitative analyzer.

The autoradiography method is based on detection of radiation with nuclear emulsions. The sensibility of the autoradiographic film is a function of exposition time, activity of the radiation target and the blackening of the photographic film (Hellmuth et al. 1993). A Kodak® X-OMAT MA film (20 μm resolution) was used with the impregnated samples and together with ^{14}C-PMMA calibration series (5.1356^{-3} to 97.535^{-3} MBq/ml activities). These patterns are used to calculate the calibration function for quantitative analyses of rock porosity (Hellmuth et al. 1993). The exposition time of rock samples and thin sections was 5 days. The obtained autoradiographies were digitalized in BMP grey level (8 bit), using transparent option and a resolution of 1200 dpi (each pixel is 21.2 μm^2) using a UMAX Power Look III scanner.

Theoretical Assumptions of Porosity Calculation

The porosity quantification is based on the assumption that optical densities on autoradiographies are proportional to the decaying isotope contents in the studied material (Hellmuth et al. 1993, Oila et al. 2005).

The rock porosity calculation using the autoradiographies comprises the following steps:

- initially all grey-levels intensities (I) and its related background (I_0) are determined digitally in several areas of the sample;
- the optic densities (D) are calculated using the Lambert-Beer law (Equation 1) and lately converted into activities (A) using Microcal Origin® software. This software provides a calibration curve based on interactive calculation using tree parameters: the k correction factor, the minimum optical density (D_0) and the maximum optical density (D_{max}) shown in equation 2 (Treutler and Freyer 1988);
- the activities are then converted to porosities using the Autoradio© software (D. Prêt, unpublished data).

$$D = -\log\left(\frac{I}{I_0}\right) \tag{1}$$

$$A = \left(\frac{-1}{k}\right)\ln\left[1 - \left(\frac{D - D_0}{D_{max}}\right)\right] \tag{2}$$

The quantitative porosity measurement is based on the assumption that the rock matrix dilutes the ^{14}C-PMMA. If the pore sizes are under the resolution of the autoradiography (usually > 0.1 μm), the major fraction of the emitted β-radiation is attenuated by the rock and the porosity calculation is applicable. The local rock porosity (ϕ) is obtained by the calculation of the ^{14}C tracer contents in an analyzed area (Equation 3):

$$\phi\% = \beta\left(\frac{A}{A_0}\right)100\% \tag{3}$$

where A is the specific activity of an individual pixel (MBq/ml), A_0 is the tracer initial specific activity (0.5 MBq/ml) and β is the correction factor to β-particles absorption from the rock showed in equation 4:

TABLE I
Location, classification, texture features and mineral contents from each sample obtained by point counting (1500 points) of thin sections. Legend: sericite (ser), chl (chlorite), calcite (cal), opaque minerals (op), hematite (hem), zircon (zr) and monazite (mz).

Sample	A	B	C	D
Location	Bloco do Butiá	Cerrito	Valdo Teixeira	Valdo Teixeira
Sampling references	BB0384 (100m depth)	Surface quarry	VT02 (58.7m depth)	VT02 (58.8m depth)
Texture	Equigranular	Porphyritic	Porphyritic	Equigranular
Classification	Perthite granite	Monzogranite	Syenogranite	Perthite granite
Primary (magmatic) minerals (volume %)				
K-feldspar	62.8	50.5	44.5	57.4
Quartz	26.4	25	33	20.6
Plagioclase	4.6	16	5.2	4
Biotite	0.6	3.5	–	–
Amphibole	3.6	3	–	–
Accessory (zr, mz)	< 1	< 1	< 1	< 1
Secondary (hydrothermal) minerals (volume %)				
	< 2 (chl, cal)	< 2 (chl, cal)	ser (2.4), cal (2.8), chl (5.5), op (0.9), hem (5.7)	ser (3.9), cal (2.8), chl (4.6), op (0.6), hem (5.8)

$$\beta = \frac{\rho_e}{\rho_0} \tag{4}$$

ρ_e is the sample density (g/cm^3) and ρ_0 is the density of MMA polymer, which is 1.18. The plot of porosity histograms allows the observation of the relative porosity frequency for individual zones of rocks. The porosity ε_t of a whole measured area is obtained from the porosity distribution by taking a weighted average (Equation 5), where $Area_n$ is the area of pixel n, and ε_n is the local porosity corresponding to pixel n.

$$\varepsilon_{total} = \frac{\sum_n Area_n \varepsilon_n}{\sum_n Area_n} \tag{5}$$

Finally, the intensity levels observed in the autoradiography are proportional to the ^{14}C-PMMA tracer contents in the rock porous spaces according to relations (1), (2) and (3). Lower intensities of grey level on the film represent 100% porosity.

Mineral Staining

After autoradiography, the primary minerals were identified on unaltered rock surfaces by staining procedure and digital processes to obtain an estimative of volume (%) of rock forming minerals in that area. As mafic minerals are highly susceptible to alteration, this technique had the aim to test the influence of different mafic contents on total porosity of unaltered rocks. Altered rocks were excluded from this process because staining techniques are similar for carbonates and mafic minerals. First, the samples were etched with hydrofluoric acid during 30 seconds, washed with distilled water, immersed in a K-ferrocyanide solution (Müller 1967) for 12 hours to stain the ferro-magnesian minerals blue and dried at room temperature for 1 hour. Second, the colored surfaces were etched with hydrofluoric acid during 30 seconds, washed with distilled water, immersed in a Na-cobaltinitrite solution (Hutchison 1974) for 1 minute and dried at room temperature for 1 hour. The latter step stain the feldspars yellow, plagioclase white and quartz grey and did not affect ferro-magnesian minerals that had already been stained.

The stained rock surfaces were digitalized in 24-bit RGB mode with high resolution in the same areas as the autoradiographies. The four colors representing different minerals were color level adjusted and thresholded using Adobe Photoshop® software to obtain a histogram of total modal contents of each color on rock surface areas. Biotite and amphibole contrast greatly with the surrounding felsic minerals and can be extracted easily. Alkali feldspar, plagioclase and quartz contents in each

sample were individualized after threshold processes on each phase.

RESULTS

Petrographic and Autoradiographic Observations

Figure 2 shows the original (not treated) rock samples (A to D) and its corresponding autoradiographies (A' to D') of the same area. From autoradiography images of impregnated samples, thin sections and SEM observations, several types of pores were identified, i.e. these data are used for porosity qualitative identification, before quantification of total and local porosity of rocks. The nomenclature of pore types follows the suggestion of Siitari-Kauppi (M. Siitari-Kauppi, unpublished data): (i) transgranular, that transect mineral grains; (ii) intergranular, represented by a connected network between grains; and (iii) intragranular (inside grains), that can be found connected to another pore type or isolated, as a residual pore. It is also important to point out that rocks usually called "unaltered" have always minor amounts of secondary minerals, as observed in the studied samples (Table I).

In sample A, porous zones observed in the autoradiography are mainly associated to transgranular and intragranular microfissures and wider patches of different grey-level intensity. The transgranular microfissure network predominates and is regularly distributed through the equigranular sample, affecting all rock forming minerals. These fissures are always unfilled or filled by a thin film of hematite. They have commonly homogeneous grey level intensity in the autoradiography and long linear forms with average 4 μm aperture. It can be better observed on alkali feldspar and quartz grains, due to volumetric predominance and lighter grey level of these minerals in the autoradiography image when compared to microfissures. Intragranular porosity is associated to linear microfissures with 2 to 3 μm aperture, usually interconnected with transgranular ones that locally coincide with cleavage plans of mafic minerals (Fig. 3A). Twin plans and perthitic exsolution structures do not correspond to porous zones (Fig. 3B) and intergranular microfissures are observed only locally. Wide patches with mean grey level intensity in the autoradiography were identified after petrographic studies as amphibole and minor amounts of biotite with 0.8 to 2 mm grain size and locally to slight sericitization of feldspars. Different grey level are observed inside the limits of mafic minerals: darker zones in the autoradiography (higher porosity) represent high density of microfissures or alteration of amphibole ($\pm$ biotite) to chlorite through cleavage planes, sometimes associated to lesser amounts of calcite, hematite and pyrite. Lighter zones of lower porosity correspond to unaltered zones of the same minerals and to quartz inclusions.

In sample B, the porphyritic texture of the rock allows us to differentiate two main sites with visual contrasting porosity intensity on autoradiography: (i) phenocrysts (alkali feldspar) and (ii) matrix (alkali feldspar, plagioclase, quartz, amphibole and biotite). Both sites comprise an interconnected network of randomly distributed trans-, intra- and intergranular microfissures affecting all rock forming minerals. Transgranular microfissures are always unfilled or partly filled by a thin film of hematite. Phenocrysts represent ample lighter areas on the autoradiography, where transgranular and intragranular microcracks occur with linear forms with average 3 μm aperture and intergranular microfissures contour grain boundaries ($\sim$ 3 μm aperture). The weak alteration of plagioclase from rapakivi mantling rims provides a bad visual estimative of alkali feldspar phenocrysts contents on autoradiography image, as alkali feldspar grains seems to be smaller (only the core is completely preserved) than they really are. The fine grained matrix provides an interconnected network of tortuous intergranular microfissures with 1.5 to 8 μm aperture (Fig. 3C), which yields a mean grey level intensity of the matrix in the autoradiography. This grey level intensity of the matrix is also provided by the presence of amphibole and biotite (in general < 0.6 mm size), usually less fractured and altered than in sample A, and in minor amounts to sericitization of plagioclase and slight alteration to chlorite and calcite. The intragranular microfissures of mafic minerals are mainly represented by opened cleavage plans with 1.3 to 4 μm width (Fig. 3D and E). Associated quartz and alkali feldspar represent always the lower porosity minerals of the matrix on the autoradiography.

Dark dots are also a well marked porosity site, which

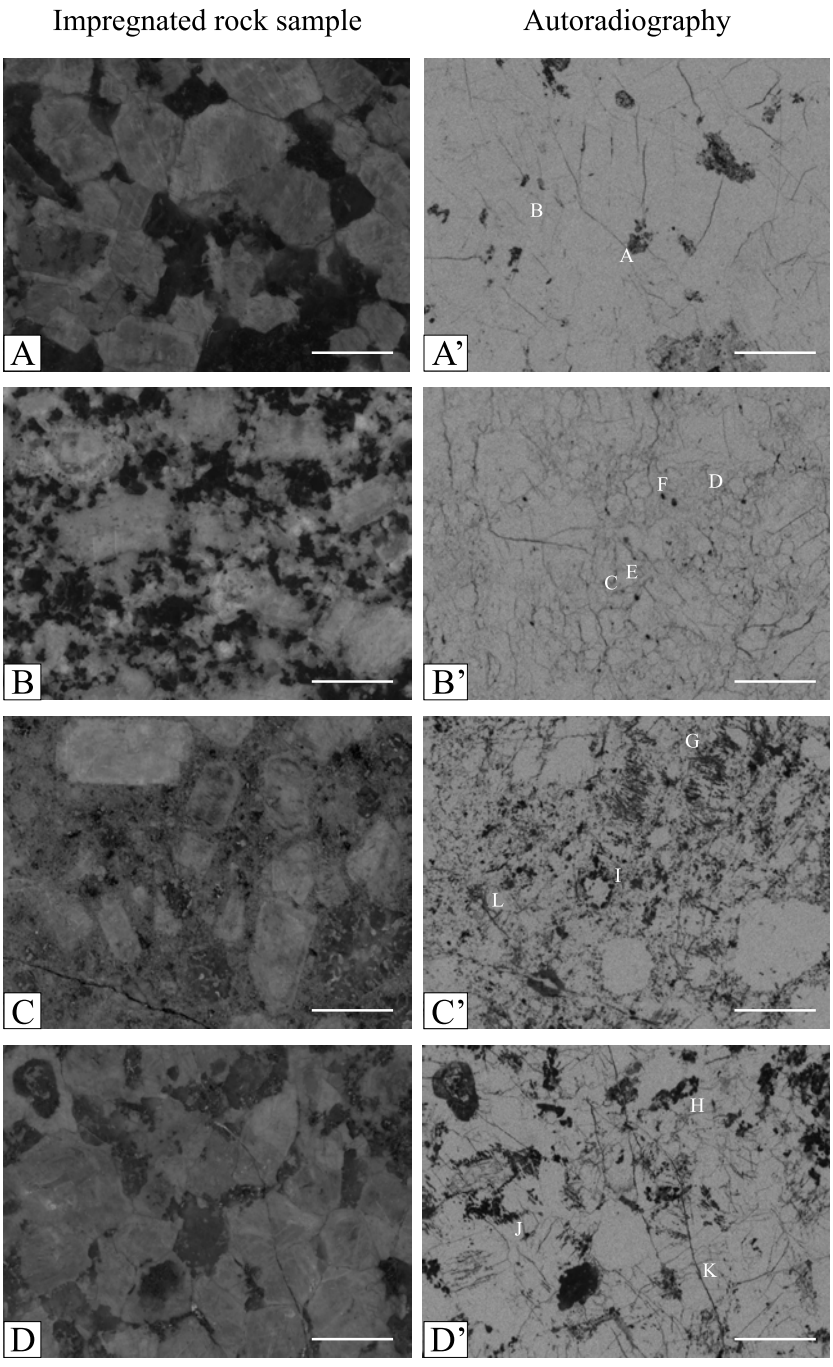

Fig. 2 – Sawed sections of ^{14}C-PMMA impregnated rock samples (left, A-D) and its corresponding autoradiographies (right, A'-D'). Area of each sample is 4.4 cm^2 and scale bars are 0.5 cm length. Samples A and B represents unaltered rocks from western border (equigranular perthite granite) and central (porphyritic monzogranite) granitic facies respectively. Samples C and D represents propylitic-altered porphyritic syenogranite (C) and equigranular perthite granite (D) from a continuous core sample from eastern border granitic facies. Autoradiographs permit to observe the spatial distribution and micrometer to decimeter heterogeneities of porous zones between different rocks. Black areas are associated to high porosity level (see text for discussion). White letters on the autoradiography (A to L) correspond to sites showed in Figure 3.

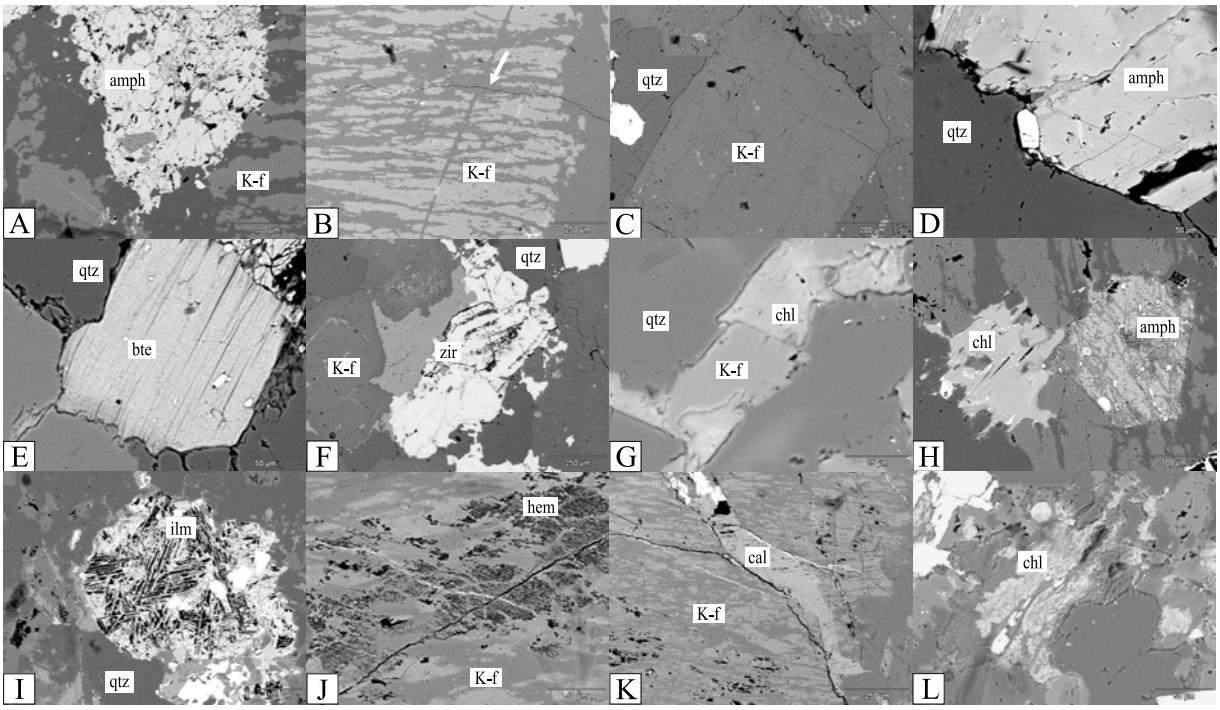

Fig. 3 – SEM images in backscattered mode (A to L) of specific sites indicated by the white letters on autoradiographies (Figure 2, A' to D'). A – intragranular microfissures in amphibole grain (sample A) that locally coincide with cleavage plans; B – perthitic exsolution texture and twin plans of alkali feldspars (sample A) do not correspond to porous sites. Note transgranular microfissure crosscutting feldspar grain (white arrow); C – fine gained matrix (sample B) yields a narrow and tortuous interconnected network of intergranular microfissures; D and E – intragranular microfissures in mafic minerals (sample B) are associated to cleavage plans of amphibole (D) and biotite (E) and intergranular ones at grain boundaries. Mafic minerals are less fractured and altered in sample B than in sample A; F – dark dots on autoradiography from sample B are associated to zircon and/or monazite crystals; G – highly connected network of tortuous intergranular microfissures from sample C, which is tighter than the same porous zones from sample B due to finer grain size of the matrix; H – pseudomorphic replacement of original biotite and amphibole for chlorite (sample D). Note that open cleavages are wider that on sample B; I – high porous zones (sample C) associated to crystallization of lath-shaped ilmenite particles; J – micro inclusions of hematite on feldspar grains (sample D); K – calcite veinlets and associated microfissures (sample D); L – very fine grained chlorite crystallizing around a thin microfissure. Key: amph (amphibole), K-f (alkali feldspar), qtz (quartz), bte (biotite), zir (zircon), ilm (ilmenite), hem (hematite), chl (chlorite) and cal (calcite).

corresponds mainly to zircon and monazite crystals (Fig. 3F).

As for the previous samples, ample light zones (low porosity) on autoradiographies of samples C and D comprise quartz and alkali feldspar. High porosity (darker) zones are mainly associated to (i) microfissures and (ii) hydrothermal alteration of original rock forming minerals. The microfissure density and width in these samples is higher than for samples A and B. It comprises a marked and connected network of trans-, intra- and intergranular pores with contrasting forms and mineral fillings, depending on rock texture.

In sample C, transgranular microfissures with 2 to 4 μm aperture have linear to slightly tortuous forms in both the rock matrix and phenocrysts (alkali feldspar and quartz). It is highly connected with a tight network of tortuous intergranular microfissures with 1 to 2 μm aperture (Fig. 3G) that follows grain boundaries. In sample D, long linear transgranular microfissures with 2.5 to 9 μm aperture (average 4 μm) predominates over all rock forming minerals, commonly connected with a network of intragranular microfissures, besides minor amounts of intergranular ones are locally observed.

Hydrothermal alteration over original (magmatic)

minerals and filling of microfissures is characteristic for samples C and D, which allows the observation of ample areas with variable grey levels (and consequently porosity) on autoradiographies. It is represented mainly by the following secondary features:

(a) pseudomorphic replacement of original mafic minerals for chlorite (Fig. 3H) and sericite (± calcite). These minerals are associated to low grey level (high porosity) areas on autoradiographies and shows wider porosity paths in open cleavages (up to 12 μm aperture) than in samples A and B. They are locally aligned or in clusters that can form rims around feldspar grains;

(b) destabilization of ilmenite (Fig. 3I), generate high porosity sites (up to 4 μm aperture) mainly in the core of the crystals, which corresponds to dark zones on the autoradiography;

(c) micro inclusions of hematite (Fig. 3J) or very fine grained chlorite ± sericite ± calcite crystallization mark commonly the compositional zoning of magmatic alkali feldspars which correspond to medium grey level intensity on autoradiography. These secondary phases were observed in either the border or the core of feldspar grains as patches or over perthite exsolution structures;

(d) calcite veinlets (Fig. 3K) with up to 150 μm width and very fine grained chlorite crystallized through infillings of microfissures (Fig. 3L) represent the alteration minerals in longer linear transgranular and in tortuous inter and intragranular porosity respectively;

(e) mafic microgranular enclaves (MME) were observed only locally on sample C. They are completely altered to chlorite ± sericite ± calcite and represents highly altered and porous zones. When present, these petrographic sites increase the porosity of the analyzed surface and comparison between original rock porosity would have no significance. For that reason, zones containing MME were excluded from total porosity quantification of that sample.

Mineralogy of Quantified Areas After Staining

The main rock-forming minerals observed in the studied samples were quartz, alkali feldspar, plagioclase and mafic minerals (amphibole and biotite). The mafic mineral contents calculated on binary (black and white) images of selected areas from samples A and B obtained after digital threshold of stained surfaces are 7.4% and 3.5% respectively (Fig. 4). Quantification of mafic mineral contents in altered samples by staining were not used, however they have similar values between porphyritic (A and D, ∼7%) and equigranular (B and C, ∼4%) samples. Tectosilicate contents (%) are Qz = 28.1 and KF = 64.5 for sample A and Qz = 27.3, KF = 58.2 and Pl = 11 for sample B.

Porosity Quantification

Total rock porosity of each sample was calculated using the Autoradio© software. In the image generated during total rock porosity calculation (Fig. 5A–D), small red points correspond to zones with very low porosity (near null) that were not computed. The corresponding total rock porosity map (Fig. 5A'–D') is obtained after transformation of the logarithmic ratio grey level of autoradiographies to a linear one, which is visually an easier way to compare between different porosity values in selected areas of the samples. However, this process of transformation generates an image with inverse tonality, when compared to the autoradiography, i.e. in this case, black represent the lowest porosity areas and white the highest porosity ones.

Calculated values of connected porosity for 4.4 cm^2 rock surfaces are 0.5% for sample A, 0.6% for sample B, 1.7% for sample C and 1.8% for sample D. The porosity histograms of rocks represented in a log-linear scale (Fig. 6) show similarities between samples with the same textural characteristics (porphyritic or equigranular). Images from samples A and D have the highest quantity of pixels with 0.25% porosity and samples B and C with 0.35% porosity respectively. Porosity curves increases up to 4% for unaltered rocks and up to 10% for altered rocks.

Microfissure sites from samples A and B shows 1.5 to 5.5% porosity, using a 3 pixel width for porosity profiles. The same sites from samples C and D can reach

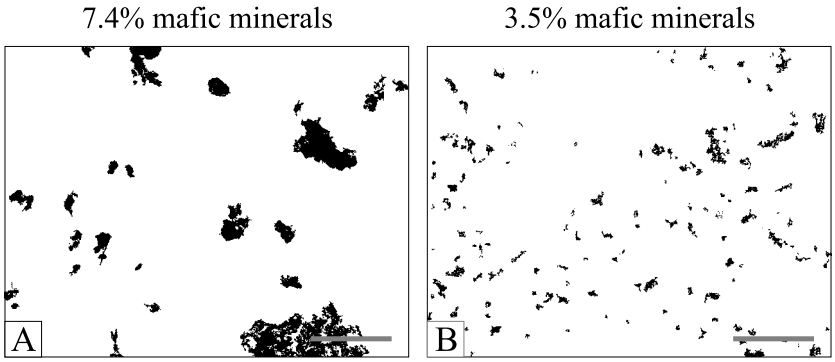

Fig. 4 – Binary (black and white) image generated by threshold of unaltered samples A (A) and B (B) using Adobe Photoshop® software after selective staining. Black corresponds to mafic minerals (amphibole and biotite) contents in each sample. Scale bars are 0.5 cm length.

6% when associated to calcite veinlets and 5 to 8.5% when very fine grained chlorite is present.

The mineral-specific porosity in all samples was estimated on the autoradiographies using rectangular areas with homogeneous grey-level zones in each identified mineral phase. It shows constant values between 0.2 to 0.4% for quartz and alkali feldspar in all samples. Average of mineral porosity in samples A and B was 1 to 1.8% for amphibole, 1.7 to 2% for biotite and 12% for accessory minerals (zircon and monazite). In samples C and D mineral sites shows porosity values up to 4.5% for calcite altering mafic minerals or feldspars, 4 to 7% for sericite + chlorite + calcite altering mafic minerals, 8% for oxide + very fine grained chlorite crystallized over feldspars, 1.5 to 5% for sericitization of feldspars, 8% for destabilized ilmenite and 14% for altered microgranular mafic enclaves.

DISCUSSION AND CONCLUSIONS

Natural microcracks in granitic rocks are commonly associated to (i) thermal contraction during cooling, (ii) stress relaxation during uplift or unroofing and (iii) tectonic deformation (Kowallis and Wang 1983). No tectonic deformation was visually recognized near sampling locations during fieldwork, however infillings of secondary veinlets can generate additional microcracks in propylitic-altered rocks.

^{14}C-PMMA porosity results of total rock calculations were compared with data obtained by the same method on granitic rocks worldwide. Unaltered, fairly and strongly altered granitic rocks show commonly 0.1 to 0.5%, 0.4 to 1% and 1 to 5% porosity respectively (Siitari-Kauppi et al. 1997, Hölttä et al. 1997, Johansson et al. 1998). Consequently, the obtained data on unaltered (0.5% to 0.6%) and propylitic-altered (1.7% to 1.8%) granitic samples from Lavras do Sul region are in agreement with the range of porosity values for similar rocks reported by other authors (Sardini et al. 2006).

Results of total rock porosity between unaltered rocks (A and B) are quite similar, if we take into account that sample B (inactive quarry) was exposed to surface alteration for a longer period of time (up to 50 years) than sample A (borehole). However, slightly differences in the weathering and the slight propylitic alteration between unaltered samples are possible. Surface exposition through time yields a low increase in total rock porosity as argued by other authors (Guillot et al. 2000, Thuro and Scholz 2003, Iñigo et al. 2000).

Some textural aspects between unaltered rocks could enable different values for the measured porosity. Porphyritic rocks from central facies have intergranular microfissures (allowed by the fine grained matrix) with high tortuosity that is not well developed in equigranular rocks from border facies. High tortuosity and constrictivity are commonly interpreted as longer pathways to fluid flows. The effect of trans- and intragranular microfissures with low tortuosity and low constrictivity in both textural rocks seems to prevail over narrow and tortuous intergranular ones. As observed in the obtained

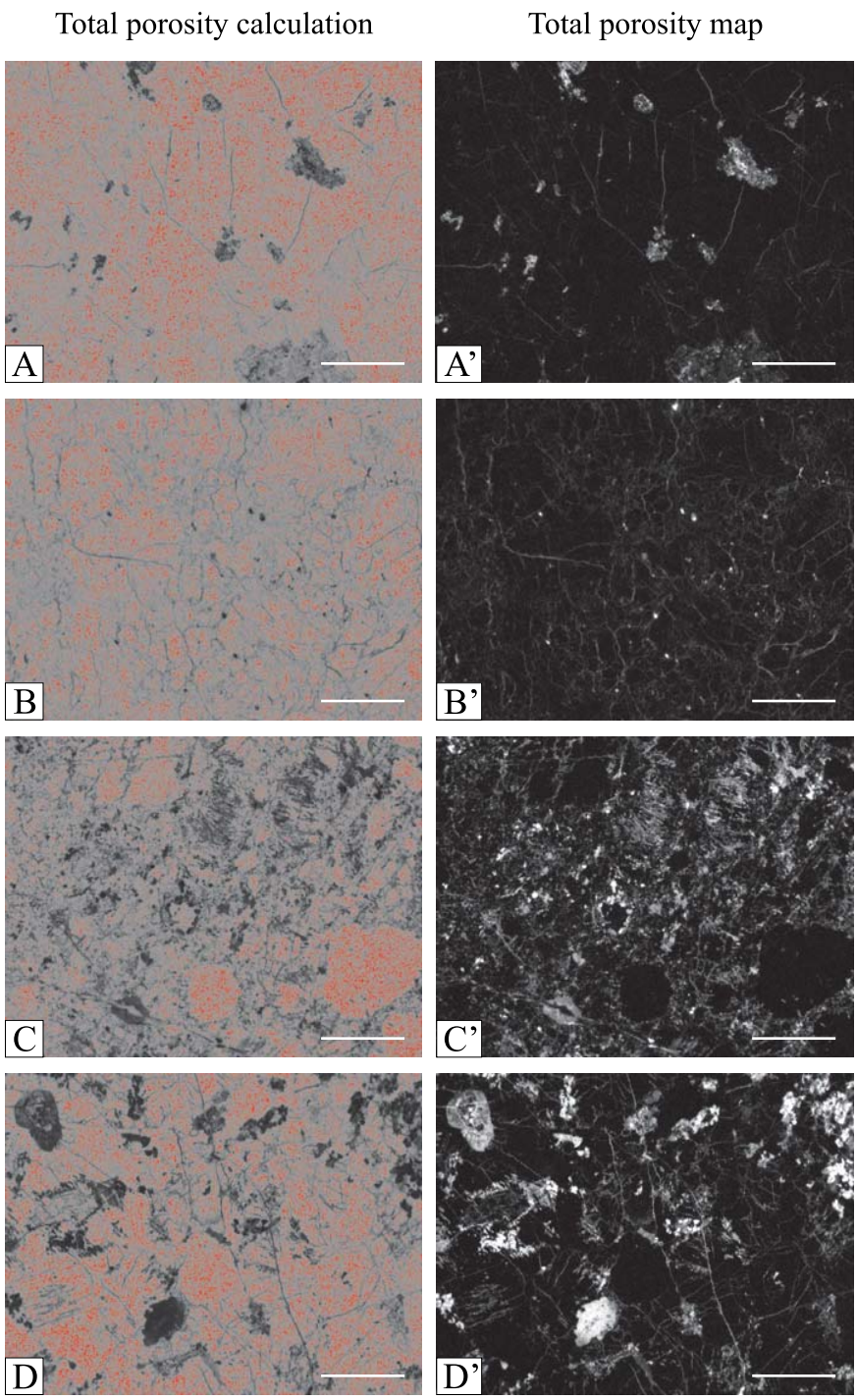

Fig. 5 – In the image generated by the Autoradio software during total porosity calculation (left, A-D), small red points correspond to near null porosity pixels that are not computed. Total porosity maps (right, A'-D') were obtained after total porosity calculation and conversion of the logarithmic-scale grey level intensities of the autoradiography to linear (0-100%) grey level intensities. The darker zones (higher porosity) of the autoradiography (black = 100% porosity) correspond to inverse tonalities (white = 100% porosity) in the total porosity maps. A to D (left) and A' to D' (right) correspond to the same image areas showed in figure 2. Scale bars are 0.5 cm length.

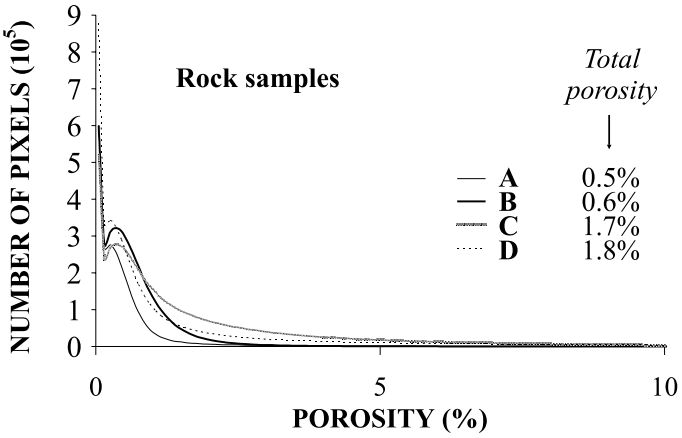

Fig. 6 – Histogram of total rock porosity (%) calculated for samples A, B, C and D. See text for discussion.

data, those different textural characteristics seem to have no effective influence on the fluid flow through very low porosity media as unaltered granitic rocks. Moreover, slight increase of the measured total porosity of sample B is expected due to its higher contents of accessory minerals (zircon and monazite), which contain radioactive elements excited during sample irradiation. Concerning mafic minerals, amphibole predominates largely over biotite. These grains are in general well preserved and differences of mafic mineral contents or extension of surface areas (in clusters or as single grains) between samples do not modify their connected (total) porosity value. Total porosity histogram for these rocks is compatible with specific porosity of individual sites, which shows predominance of up to 4% porosity. The range of porosity values for mafic minerals increases linearly with open cleavages, intragranular microfissures and chloritization contents of these petrographic sites.

The main difference between samples C and D comprises also the rock texture. Both samples were collected in the same depth (borehole) and for that reason they were exposed to identical events of primary and secondary porosity formation (i.e. microcrack evolution, hydrothermal alteration and weathering). As for unaltered rocks, the occurrence of intergranular microfissures did not allowed high variations in the measured porosity between samples C and D (1.7 and 1.8%). Histograms of total porosity have higher maximal values than for unaltered rocks, and porosity values vary up to 10%. These data agree with porosity calculated for individual petrographic sites. Opened cleavages, carbonate and chlorite veinlets and diffuse alteration (chloritization, sericitization) of original minerals allow an effective increase in total porosity of these samples in comparison to values obtained for unaltered rocks.

From the bulk results we can consider the following aspects:

- spatial distribution of porosity values is dependent on the mineralogy (either primary or secondary), as reported in previous papers (Oila et al. 2005, Sardini et al. 2006);
- variable porosity values within a single mineral grain is dependent on its alteration degree or imperfect development of crystal growth;
- undeformed quartz and unaltered alkali feldspar have null to very weak porosity values and feldspar sericitization (weathered or hydrothermal) increases its porosity and total porosity of rocks;
- cleavage (mafic minerals), grain boundaries, compositional zonation (rapakivi, perthite), microcracks, degree of alteration and accessory minerals with radioactive elements are representative of distinct porosity values;

- high mafic mineral contents and clusters increase conditions to form secondary porosity if they are previously altered or fractured.

The results obtained in this study shows that original porosity of granitic rocks with different textures (samples A and B) have no significant influence on the differences of diffusion (width) of later phyllic alteration halos around veins observed during field works between central and border facies granitoids.

Secondary porosity represented by propylitic-altered rocks (samples C and D) has higher porosity values either in total or specific mineral quantifications between different rock textures. Propylitic alteration commonly develops in response to low water/rock ratio in ample areas of hydrothermal systems (Berger and Velde 1992, Titley 1982) and phyllic alteration, on the contrary, needs high fluid/rock ratio in narrow zones of active fluid flow (fractures, veins) to develop.

Early and widespread propylitic alteration in the studied area may have provided additional porosity for rocks due to fluid interaction (Holl et al. 1997) through cleavage plans, microcracks and secondary minerals of higher porosity prior to phyllic alteration stage near quartz veins, but the variability of diffusion width observed on alteration halos between granitic facies might be produced during phyllic alteration. If true, central and border facies were influenced by different fluid/rock ratio or fluid composition during phyllic alteration stage. That hypothesis must also consider variations in the hydrothermal products, timing between granitic facies emplacement and/or paleoenvironment of rocks (depth, superimposing alteration stages, tectonic deformation and location within the granitic body). Moreover, microgranular mafic enclaves (MME) commonly found in the border facies are also highly porous zones that if present can locally contribute to increase the hydrothermal fluid diffusion.

The ^{14}C-polymethylmethacrylate (^{14}C-PMMA) impregnation method, coupled with petrographic (optical and through SEM) observations and digital image processing provides a valuable methodology to identify and quantify the porosity heterogeneities in hydrothermally altered rocks and specific minerals. The modeling of fluid flows and evolution of porosity in different stages during hydrothermal alteration is also possible. The initial porosity (fairly altered, unaltered) and porosity generated during early alteration stages (propylitic) of these granitic rocks obtained by the ^{14}C-PMMA method should be compared with other hydrothermal stages/ environments (phyllic alteration, around vein selvages) within the same locations to test the observation of porosity evolution until its final stages. The recognition and quantification of the connective network and of alteration products observed in this study can be also used as a data basis for calculation of mass balance of alteration.

ACKNOWLEDGMENTS

This study was partly funded by Programa de Apoio de Núcleos de Excelência (PRONEX) / Fundação de Amparo à Pesquisa do Estado do Rio Grande do Sul (FAPERGS) – project 04/0825.3. The authors wish to thank Companhia Brasileira do Cobre (CBC) and Companhia Riograndense de Mineração (CRM) for providing access to drill core samples. Everton M. Bongiolo also thanks Conselho Nacional de Desenvolvimento Científico e Tecnológico (CNPq) for Ph.D. scholarship and Coordenação de Aperfeiçoamento de Pessoal de Nível Superior – Comité d'Évaluation de la Coopération Universitaire avec le Brésil (CAPES-COFECUB) project (349-01/2003).

RESUMO

Este trabalho é uma aplicação do método ^{14}C-polimetilmetacrilato na comparação da evolução da porosidade entre granitos não alterados e propilitizados, utilizando amostras da região de Lavras do Sul, Brasil. Este método, quando associado a análises por petrografia ótica, eletrônica e processamento digital de imagens tem a vantagem de fornecer, além da porosidade total, a quantificação e identificação da porosidade em locais específicos das rochas. A partir da petrografia foi possível identificar e quantificar os diferentes tipos de poros presentes nas rochas (microfraturas, limites de grãos, alteração de minerais, etc). Os resultados mostram que granitos não alterados têm porosidade de 0,5 a 0,6% e granitos propilitizados 1,7 a 1,8%, com valores semelhantes para rochas de texturas diferentes. A porosidade das rochas alteradas aumenta, principalmente, devido à maior porosidade dos minerais neoformados como clorita, calcita e sericita e de microfraturas. Observações de campo mostram que halos de alteração fílica, posteriores à

propilitização, são maiores em rochas equigranulares do que em porfiríticas, o que não pode ser explicado pelo valor semelhante da porosidade original dessas rochas. A difusão diferencial da alteração fílica foi, portanto, condicionada por variações estruturais ou da razão fluido/rocha entre as facies equigranular e porfirítica durante este estágio hidrotermal posterior.

Palavras-chave: quantificação de porosidade, método ^{14}C-polimetilmetacrilato, porosidade de granitos, alteração hidrotermal, alteração propilítica, Lavras do Sul.

REFERENCES

BERGER G AND VELDE B. 1992. Chemical parameters controlling the propylitic and argillic alteration process. Eur J Mineral 4: 1439–1454.

DUBOIS C, COUCHOT P, ALVAREZ CALLEJA A, BOEGLIN E AND CHAMBAUDET A. 1998. Specific mercury porosimetry for low-porosity materials. Meas Sci Technol 9: 2016–2022.

GASTAL MCP AND LAFON JM. 1998. Gênese e evolução dos granitóides metaluminosos de afinidade alcalina da porção oeste do escudo Sul-riograndense: Geoquímica e isótopos de Rb-Sr e Pb-Pb. Rev Bras de Geocienc 28: 11–28.

GUILLOT L, SIITARI-KAUPPI M, HELLMUTH K-H, DUBOIS C, ROSSY M AND GAVIGLIO P. 2000. Porosity changes in a granite close to quarry faces: quantification and distribution by ^{14}C-MMA and Hg porosimetries. Eur Phys J AP 9: 137–146.

HELLMUTH K-H, SIITARI-KAUPPI M AND LINDBERG A. 1993. Study of porosity and migration pathways in crystalline rocks by impregnation with ^{14}C-polymethylmetacrylate. J of Contam Hydrol 13: 403–418.

HOLL A, ALTHAUSE E, LEMPP C AND NATAU O. 1997. The petrophysical behavior of crustal rocks under the influence of fluids. Tectonoph 275: 253–260.

HOLTTA P, SIITARI-KAUPPI M, HAKANEN M, HUITTI T, HAUTOJARVI A AND LINDBERG A. 1997. Radionuclide transport and retardation in rock fracture and crushed rock column experiments. J of Contam Hydrol 26: 135–145,

HUTCHISON CS. 1974. Laboratory handbook of petrographic techniques, J Wiley & Sons, New York, USA, 527p.

IÑIGO AC, VICENTE MA AND RIVES V. 2000. Weathering and decay of granitic rocks: its relation to their pore network. Mech Mater 32: 555–560.

JOHANSSON H, SIITARI-KAUPPI M, SKÅLBERG M AND TULLBORG EL. 1998. Diffusion pathways in crystalline rock-examples from Äspö-diorite and fine-grained granite. J of Contam Hydrol 35: 41–53.

KOWALLIS BJ AND WANG HF. 1983. Microcrack study of granitic cores from Illinois deep borehole UPH-3. J Geophys Res 88: 7373–7380.

MÜLLER G. 1967. Methods in sedimentary petrology. In: ENGELHARDT WV ET AL. (Eds), Sedimentary petrology, v. I, Schweizerbart'sche, Stuttgart, p. 163–167.

NARDI LVS AND LIMA EF. 1985. A Associação Shoshonítica de Lavras do Sul, RS. Rev Bras de Geocienc 15: 139–146.

NARDI LVS AND LIMA EF. 2000. O magmatismo Shoshonítico e Alcalino da Bacia do Camaquã – RS. In: HOLZ M AND DE ROS LF (Eds), Geologia e Estratigrafia do Rio Grande do Sul. Editora Gráfica da UFRGS, Porto Alegre, RS Brasil, p. 119–131.

OILA E, SARDINI P, SIITARI-KAUPPI M AND HELLMUTH K-H. 2005. The ^{14}C-polymethylmetacrylate (PMMA) impregnation method and image analysis as a tool for porosity characterization of rock-forming minerals. In: HARVEY PK ET AL. (Eds), Petrophysical properties of crystalline rocks. Geol Soc London S Publ 240: 335–342.

REMUS MVD, HARTMANN LA, MCNAUGHTON NJ AND GROVES DI. 2000. Distal Magmatic-Hydrothermal Origin for the Camaquã Cu (Au-Ag) and Santa Maria Pb, Zn (Cu-Ag) Deposits, Southern Brazil. Gondwana Res 3: 155–174.

SARDINI P, SIITARI-KAUPPI M, BEAUPORT D AND HELLMUTH K-H. 2006. On the connected porosity of mineral aggregates in crystalline rocks. Am Miner 91: 1069–1080.

SCHILD M, SIEGESMUND S, VOLLBRECHT A AND MAZUREK M. 2001. Characterization of granite matrix porosity and pore-space geometry by *in situ* and laboratory methods. Geophys J Int 146: 111–125.

SIITARI-KAUPPI M, LINDBERG A, HELLMUTH K-H, TIMONEN J, VÄÄTÄINEN K, HARTIKAINEN J AND HARTIKAINEN K. 1997. The effect of microscale pore structure on matrix diffusion – a site specific study of tonalite. J of Contam Hydrol 26: 147–158.

THURO K AND SCHOLZ M. 2003. Deep weathering and alteration in granites – a product of coupled processes. In: PROCEEDINGS OF THE INTERNATIONAL CONFERENCE ON COUPLED T-H-M-C IN GEOSYSTEMS: Fundamentals, Modelling, Experiments and Application, 1, Stockholm, Royal Institute of Technology (KTH), p. 1–6.

TITLEY SR. 1982. The style and progress of mineralization and alteration in porphyry copper systems. In: TITLEY SR (Ed), Advances in geology of the porphyry copper deposits, Southwestern North America. Tucson, University of Arizona Press, Arizona, p. 93–166.

TREUTLER HC AND FREYER K. 1988. Die quantitative autoradiographie als methode der radioaktivitatsmessung. Isotopenpraxis 24: 220–223.

YUE ZQ, SHANG YJ, HU RL AND TU XB. 2004. Five test methods for porosity of completely decomposed granite in Hong Kong. Int J Rock Mech Min Sci 41(3):1–8.